

D. Ducreux
I. Huynh
P. Fillard
J. Renoux
M. C. Petit-Lacour
K. Marsot-Dupuch
P. Lasjaunias

Brain MR diffusion tensor imaging and fibre tracking to differentiate between two diffuse axonal injuries

Received: 15 October 2004
Accepted: 25 March 2005
Published online: 23 June 2005
© Springer-Verlag 2005

D. Ducreux (✉) · I. Huynh
J. Renoux · M. C. Petit-Lacour
K. Marsot-Dupuch · P. Lasjaunias
Department of Neuroradiology, CHU de
Bicêtre, Paris XI University, 78 rue du
General Leclerc, 94270 Le Kremlin Bicêtre,
France
E-mail: denis.ducreux@bct.ap-hop-paris.fr
Tel.: +33-1-45212601
Fax: +33-1-45212317

P. Fillard
Department of Computer Science,
University of North Carolina, Chapel Hill,
North Carolina, USA

Abstract We report here two cases of diffuse axonal injury (DAI) studied by MR diffusion tensor imaging (DTI) and fibre tracking (FT) focused on the corpus callosum. In one case, DTI and FT pattern matched the diagnosis of broken white matter tracts. In the other case there was a discrepancy between DTI and FT data that showed unaltered white matter tracts with the presence of intra-cellular oedema. These data suggested that DTI and FT are able to differentiate between traumatic cytotoxic oedema and broken fibres in the case of DAI.

Introduction

Diffuse axonal injury (DAI) is one of the most frequent types of primary injury that can be seen in patients with severe head trauma [1]. It occurs in approximately 50% of all head trauma cases and is characterized clinically by loss of consciousness starting at the moment of impact. Pathologically, multiple, bilateral, small, focal lesions throughout the white matter, mainly at the grey/white junction, are seen. The lesions are located in three characteristic areas: corpus callosum, brain stem (in particular the dorsolateral region and the cerebral peduncle), and lobar white matter (frontal and temporal). Corpus callosum lesions are located mainly in the posterior body and splenium; occasionally, the entire corpus callosum is involved. As MRI is the modality of

choice for demonstrating DAI [2], we investigated the use of diffusion tensor imaging (DTI) and brain white matter fibre tracking (FT), focused on the corpus callosum in two patients with severe head injury, to assess the axonal disruption usually observed in this disease.

Cases report

Patient 1

A 19-year-old man was admitted to our intensive care unit after a car crash injury. The clinical examination found a Glasgow score of 7 out of 15, confusion, mild left hemiparesis, and cerebellar ataxia. An MR brain study

was performed with a 1.5-T MR Scanner (Sonata, Siemens), 2 days after his admission, with sagittal T1-weighted images (430/8 ms TR/TE), coronal T2-weighted gradient echo (830/33 ms TR/TE), axial fluid-attenuated inversion recovery (FLAIR, 8740/104/2200 ms TR/TE/TI) and axial EPI diffusion tensor imaging (DTI, 4900/85 ms TR/TE) with diffusion gradients set in six non-collinear directions using two b values ($b=0$ and $1,000 \text{ s/mm}^2$) (field of view $24 \text{ cm} \times 24 \text{ cm}$; image matrix 128×128 ; 30 slices with section thickness 4 mm , nominal voxel size $1.875 \text{ mm} \times 1.875 \text{ mm} \times 4 \text{ mm}$, number of signal average 3). The DTI directions were as follows: $[(1/\sqrt{2}, 0, 1/\sqrt{2}); (-1/\sqrt{2}, 0, 1/\sqrt{2}); (0, 1/\sqrt{2}, 1/\sqrt{2}); (0, 1/\sqrt{2}, -1/\sqrt{2}); (1/\sqrt{2}, 1/\sqrt{2}, 0); (-1/\sqrt{2}, 1/\sqrt{2}, 0)]$ providing the best precision in the tensor component when six directions are used [3]. The duration of diffusion-weighted imaging was 1 min 40 s (brain) per patient study. The DTI raw images were analysed with DPTools software (<http://fmri-tools.hd.free.fr>). The six elements (Dxx, Dyy, Dzz, Dxy, Dxz and Dyz) for each voxel calculated from six images obtained by applying diffusion-sensitising gradients in the six non-collinear directions (xx, yy, zz, xy, xz and yz), in addition to a non-diffusion-weighted image, were diagonalized to compute the eigenvalues ($\lambda_1, \lambda_2, \lambda_3$) of the diffusion tensor matrix. Then, the apparent diffusion coefficient (ADC) was computed using $\text{ADC} = (\lambda_1 + \lambda_2 + \lambda_3)/3$, and the fractional anisotropy (FA) was computed using:

$$\text{FA} = \sqrt{\frac{3}{2}} \frac{\sqrt{(\lambda_1 - \bar{D})^2 + (\lambda_2 - \bar{D})^2 + (\lambda_3 - \bar{D})^2}}{\sqrt{\lambda_1^2 + \lambda_2^2 + \lambda_3^2}}$$

The FA values around 1 are totally anisotropic; FA values around 0 are totally isotropic [3].

In addition to the two-dimensional parametric colour maps processed by previous methods, three-dimensional

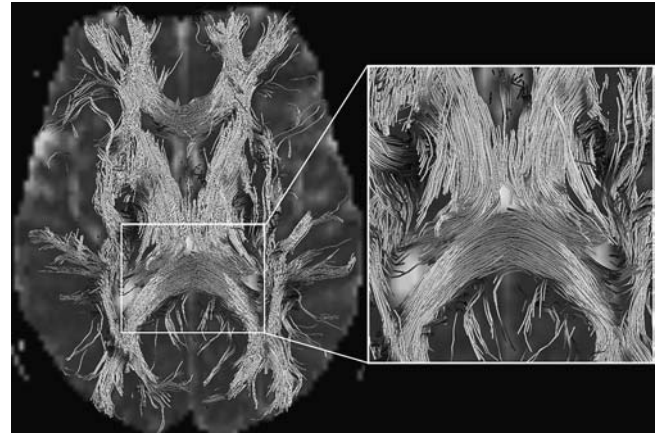
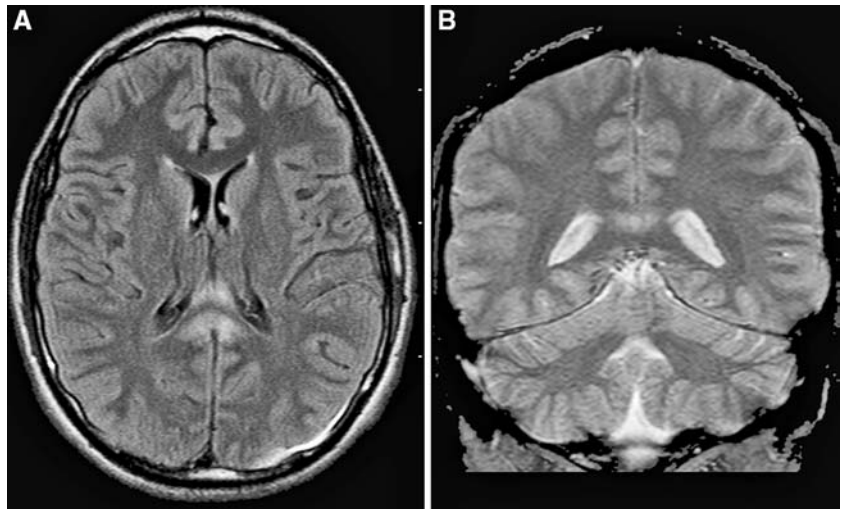


Fig. 1 Reconstruction of white matter fibres of the brain superimposed over DTI b_0 images. The fibres are colour-coded for direction: *blue fibres* are cranio-caudal, *green fibres* are antero-posterior and *red fibres* are transverse. Normal pattern of the white matter fibres inside the genu (anterior) and splenium (posterior) part of the corpus callosum, with anterior efferent forceps fibres. Note that the cortico-spinal tract appears in *blue* on the posterior part of the internal capsule

white matter fibre tract maps was created and co-registered on these maps using a special algorithm previously described [4, 5]. Results of our FT method performed on a normal volunteer corpus callosum are presented in Fig. 1.

There were, on the T2-weighted and FLAIR images, multiple, abnormal, high intensity signal lesions in centra ovale, corpus callosum (splenium), and pons white matter, without hypointense areas on T2* sequences (see Fig. 2). MRI also showed a left parietal sub-dural haematoma. As we focused the study on corpus callosum lesions, we drew two regions of interest (ROIs) of 88 mm^2 (25 pixels) on the DTI b_0 : one on the

Fig. 2 Patient 1: axial FLAIR (a) and coronal T2* (b) images centred on the corpus callosum. Hyperintense area in T2* and FLAIR on the splenium without T2* hypointense area (no magnetic susceptibility effect) that suggests the presence of oedema



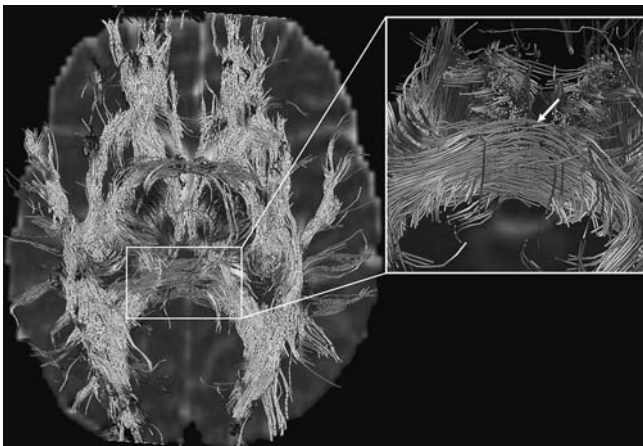
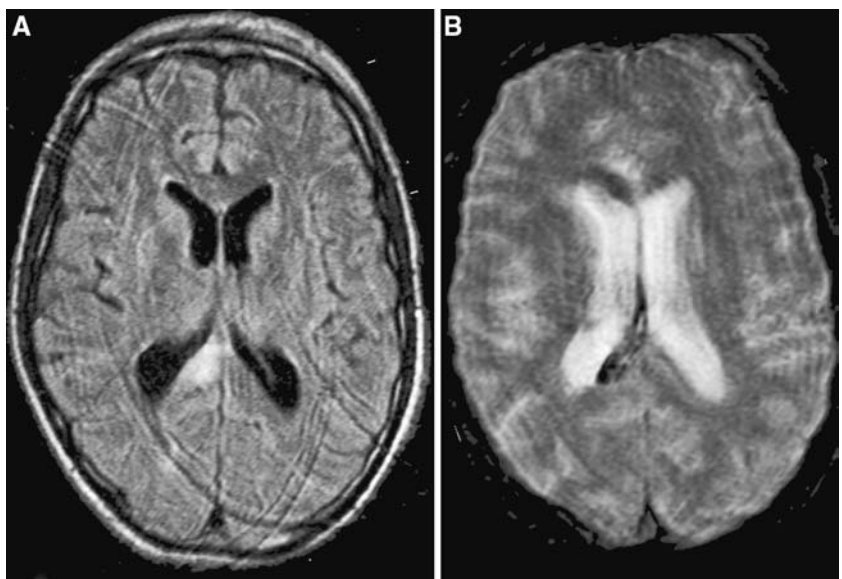


Fig. 3 Patient 1: reconstruction of brain white matter fibres superimposed over DTI b_0 images. The fibres are colour-coded for direction: *blue fibres* are cranio-caudal, *green fibres* are antero-posterior and *red fibres* are transverse. Splenium fibres are slightly warped in the superior part and widened (*arrow*). There are no broken fibres

abnormal area that matched the abnormal area in FLAIR and one on the normal part of the splenium. The ADC values in the abnormal area were slightly decreased ($0.723 \pm 0.01 \times 10^{-3} \text{ mm}^2/\text{s}$) when compared with the normal area ($0.77 \pm 0.01 \times 10^{-3} \text{ mm}^2/\text{s}$), and FA values were decreased ($\text{FA} = 0.38 \pm 0.08$) (see Fig. 2) when compared with the normal area (0.77 ± 0.08).

The FT of the brain showed an unexpected, unaltered, pattern of the white matter tracts, especially on the corpus callosum splenium, with some mildly warped fibres in areas of abnormal FLAIR signal. No fibre disruption was seen (see Fig. 3), and these data ruled out the presence of broken fibres.

Fig. 4 Patient 2: axial FLAIR (a) and T2* (b) images centred on the corpus callosum. The FLAIR hyperintense areas that are hypointense on T2* and FLAIR on the genu and splenium suggest the presence of magnetic susceptibility effect (methaemoglobin)



The patient's condition rapidly improved, and he left the intensive care unit 1 week after admission.

Patient 2

Another 19-year-old man was admitted to our intensive care unit after a car crash injury. The clinical examination found a Glasgow score of 4 out of 15, with bilateral myosis, decortication abnormal movements, and priapism. The MR study was performed 1 day after admission, with same sequences protocol as described above.

There were, on the T1-weighted and FLAIR images, multiple, abnormal, high intensity signal lesions in centra ovale, corpus callosum (splenium), and pons white matter, which were hypointense on T2* sequences (see Fig. 4). These data suggested a magnetic susceptibility effect of methaemoglobin. We drew on the DTI b_0 images two ROIs of 88 mm^2 (25 pixels), one on the patient's abnormal corpus callosum (splenium) area that matched the abnormal one in FLAIR and one on the normal part of the splenium. The ADC values were increased ($1.11 \pm 0.03 \times 10^{-3} \text{ mm}^2/\text{s}$), and FA values were decreased ($\text{FA} = 0.33 \pm 0.08$) when compared with the normal area ($\text{ADC} = 0.782 \pm 0.01$; $\text{FA} = 0.74 \pm 0.12$).

The FT of the brain showed the expected, altered, pattern of the white matter tracts, on the anterior genu and posterior splenium of the corpus callosum, with disrupted and warped fibres (see Fig. 5) that suggested diffuse broken axonal fibres.

The patient's condition had not improved by 1 week after the onset, with global spastic hypertonia and neurovegetative state.

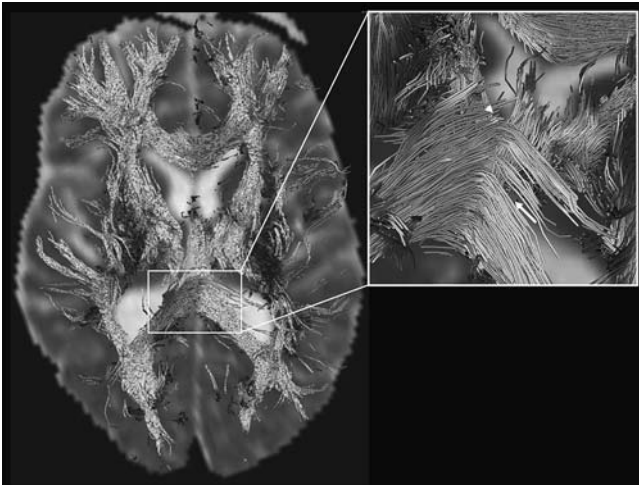


Fig. 5 Patient 2: reconstruction of brain white matter fibres superimposed over DTI b_0 images. The fibres are colour-coded for direction: *blue fibres* are cranio-caudal, *green fibres* are antero-posterior and *red fibres* are transverse. Splenium and genu fibres are widened and warped in the left segment (*arrow*) and broken in the right segment (*arrowhead*)

Discussion

The pathophysiology and dynamic mechanisms that lead to DAI are still uncertain [6]. Current opinion is that corpus callosum injury is mediated by rotationally induced shear-strain forces and/or impact against the free margin of the falx. In patients who have suffered mild rotational acceleration/deceleration the lesions may be confined to the white matter of the frontal and temporal lobes at the grey/white matter junction, owing to different inertial response of the two components with disruption of axons from the neuronal cell bodies.

MRI is the modality of choice for demonstrating DAI [2]. The lesions appear as small, punctate areas of abnormal signal, mainly T2 hyperintense, with, however, some paramagnetic effects such as T2 shortening, due to haemosiderin or T1 shortening, due to methaemoglobin when haemorrhagic components are present. Their sizes usually vary from 5 mm to 15 mm, and they are oval or elliptical with the long axis parallel to the direction of the involved axonal tracts. MRI may underestimate the true extent of DAI, because the abnormal signal can be seen only where axonal disruption is confluent enough to allow visualization. To improve MRI diagnosis accuracy in DAI, we investigated the use of DTI MR sequences.

The diffusion-weighted (DW) and DT images provide information on the mobility of water molecules in tissue. It is a widely accepted and utilized method for detecting acute ischemic brain injury [7, 8]. Highly mobile extra-cellular water shifts into the intra-cellular compartment, generating 'cytotoxic oedema' during the early stage of

arterial stroke [8]. Movement of water is more restricted in the intra-cellular environment, resulting in hyperintensity on DW images, with decreased ADC values. Indeed, decreased ADC values reflect intra-cellular oedema and increased ADC values correspond to an increase in the extra-cellular space (vasogenic oedema). Thus, diffusion-weighted imaging (DWI) potentially distinguishes between cytotoxic and vasogenic oedema [8]. It has been shown that water diffusion in biological tissue is highly dependent on the ratio of extra-cellular to intra-cellular space, and it is greater in the extra-cellular space than in the intra-cellular space. The importance of the ratio of extra-cellular to intra-cellular space in determining water diffusivity has been noted in acute cerebral ischaemia, in which decreased extra-cellular to intra-cellular volume ratio is thought to be the dominant, mechanism underlying ADC reduction [9]. Pathophysiological hypotheses rely on oedema in acute and/or subacute stage [1, 2, 6], eventually associated with petechial haemorrhage.

DTI is a special MRI technique that measures the translation of extra-cellular water molecules among the white matter fibres [10], using directional evaluation of the water diffusivity (diffusion anisotropy) due to its scalar properties. The FA, a useful parameter derived from DTI computations and used for FT purposes, has been reported to be more sensitive than ADC in detecting abnormal brain areas in special diseases such as multiple sclerosis [11]. Moreover, FA, combined with tensor fields estimation, is used to reconstruct three-dimensional white matter fibre tracts [4] based on similarities between neighbouring voxels in the shape (quantitative diffusion anisotropy measures) and orientation (principal eigenvector map evaluated by the tensor field) of the diffusion ellipsoid. Factors affecting the shape of the apparent diffusion tensor in the white matter include the density of fibres, the degree of myelination, the average fibre diameter and the directional similarity of the fibres in the voxel [4]. Then, it is possible to access the fibre connectivity [12].

In patient 1 the discrepancy between decreased ADC and FA measurements in the abnormal area of the splenium was associated with a quite normal aspect of the computer-generated white matter tracts on the FT reconstructions, despite some slightly altered tracts that appeared warped by oedema. The ADC findings suggested that oedema was intra-cellular (decreased ADC values). However, FA is sensitive to extra-cellular oedema, which involves the white matter tracts, and FA is used to reconstruct white matter tracts by FT. The FT algorithm links voxels of similar FA value, then reflects the anatomical organization of white matter tracts regardless of the extra-cellular water quantity. Using FT, one can only indirectly assess extra-cellular water by viewing the shape of the white matter tracts, i.e. broken, narrowed or warped. In patient 1, intra-cellular water

did not alter the shape of the tracts. Conversely, some extra-cellular oedema may have warped a few splenium fibres without breaking them, as suggested by the slightly decreased ADC values found in that area and by the results of the FT reconstruction. These observations of quite unchanged splenium fibres may be explained by the FT algorithm we used: neighbouring voxels with decreased FA values may be interpreted by our FT algorithm as continuous tracts if the difference between the voxels is below the thresholding condition of the algorithm (here 0.17). If this FT algorithm was applied in patient 1, the FA differences between two splenium voxels were too small to break the fibre reconstruction. Conversely, in patient 2, the FA differences were sufficient to 'break' the fibre reconstructions, as seen in Fig. 5.

What was unexpected in patient 1 was the presence of intra-cellular oedema in the corpus callosum splenium that did not break the computer-generated fibre shape using the FT reconstruction. These data sug-

gested that the FT method we used produced white matter tract reconstructions even with abnormal FA values and may reflect the 'integrity' of these tracts. This 'integrity' might be involved in patients' clinical outcomes, as we observed in patient 1. We need more cases so that we can definitely assess this hypothesis. FT is an emerging new technique that may help radiologists to visualize normal or warped tracts and may contribute to the assessment of the integrity of white matter fibres.

Conclusion

The combination of DTI and FT provides specific information about the integrity of white matter tracts (in DAI) that may help the radiologist to differentiate between oedema and fibre disruption. Larger numbers of patients are needed so that this finding can be confirmed.

References

1. Wang H, Duan G, Zhang J, Zhou D (1998) Clinical studies on diffuse axonal injury in patients with severe closed head injury. *Chin Med J (Engl)* 111:59–62
2. Atlas SW (ed) (1996) *Magnetic resonance imaging of the brain and spine*, 2nd edn. Lippincott-Raven, Pennsylvania, USA
3. Basser P, Pierpaoli C (1998) A simplified method to measure the diffusion tensor from seven MR images. *Magn Reson Med* 39:928–934
4. Westin CF, Maier SE, Mamata H, Nabavi A, Jolesz FA, Kikinis R (2002) Processing and visualization for diffusion tensor MRI. *Med Image Anal* 6:93–108
5. Fillard P, Gerig G (2003) Analysis tool for diffusion tensor MRI. *MICCAI* 2:967–968
6. Holbourn AHS (1943) Mechanics of head injuries. *Lancet* 2:438–441
7. Le Bihan D (1991) Molecular diffusion nuclear magnetic resonance imaging. *Magn Reson Q* 7:1–30
8. Provenzale JM, Sorensen AG (1999) Diffusion-weighted MR imaging in acute stroke: theoretic considerations and clinical applications. *AJR Am J Roentgenol* 173:1459–1467
9. Latour LL, Svoboda K, Mitra PP, Sotak CH (1994) Time-dependent diffusion of water in a biological model system. *Proc Natl Acad Sci U S A* 91:1229–1233
10. Basser P, Pierpaoli C (1996) Microstructural and physiological features of tissues elucidated by quantitative-diffusion-tensor MRI. *J Magn Reson* 111:209–219
11. Tievsky AL, Ptak T, Farkas J (1999) Investigation of apparent diffusion coefficient and diffusion tensor anisotropy in acute and chronic multiple sclerosis lesions. *AJNR Am J Neuroradiol* 20:1491–1499
12. Basser PJ (1998) Fibre-tractography via diffusion tensor MRI (DTMRI). In: *V1th ISMRM*, Sydney, Australia, p 1226